Chapter 2

Realizing TM_1 mixing in the minimal seesaw model using S_4 symmetry and its implication on resonant leptogenesis

We introduce an S_4 flavour symmetric model in a minimal seesaw framework which results in mass matrices that lead to TM_1 mixing. Minimal seesaw is realized by adding two right-handed neutrinos to the Standard Model. The model predicts Normal Hierarchy (NH) for neutrino masses. Using the constrained six-dimensional parameter space, we have evaluated the effective Majorana neutrino mass, which is the parameter of interest in neutrinoless double beta decay experiments. The possibility of explaining baryogenesis via resonant leptogenesis is also examined within the model. A non-zero, resonantly enhanced CP asymmetry generated from the decay of right-handed neutrinos at the TeV scale is studied, considering flavour effects. The evolution of lepton asymmetry is discussed by solving the set of Boltzmann equations numerically and obtain the value of baryon asymmetry to be $|\eta_B| = 6.3 \times 10^{-10}$.

2.1 Introduction

Neutrinos, for a long time, have created an atmosphere of uncertainty among physicists with their properties and pose a challenge to the Standard Model of particle physics. Various neutrino oscillation experiments have determined that neutrino masses are small with large mixing [1–6]. The absence of the right-handed counterpart of the neutrinos within the Standard Model suggests we must go beyond the Standard Model to accommodate the neutrino properties.

Numerous frameworks beyond the standard model can explain the origin of neutrino masses, for instance, the seesaw mechanism [7–9], radiative seesaw mechanism [10], models based on extra dimensions [11, 12], and other models. Here, we consider a minimal seesaw mechanism, the extension of SM with two right-handed neutrinos, that can explain the origin of neutrino masses and that of the Baryon Asymmetry of the Universe (BAU) through leptogenesis [13]. In leptogenesis, the generation of baryon asymmetry involves the conversion of lepton asymmetry, obtained from the CP-violating decay of the heavy right-handed neutrinos, via the sphaleron processes [14]. It has been reported in [15] that the mass scale $\mathcal{O}(10^9)$ for the right-handed neutrino is needed to explain the observed BAU. This mass scale, however, can be lowered if the mass of right-handed neutrinos is almost degenerate. In the case of an almost degenerate mass scale for right-handed neutrinos, CP-violating effects become resonantly enhanced, and at a relatively lower mass scale (TeV scale), enough lepton asymmetry can be generated to explain BAU. Such a situation is termed Resonant leptogenesis [16]. Furthermore, over time, a lot of attention has been given to the investigation of the origin of neutrino flavour mixing. Among various possibilities, tri-bimaximal mixing (TBM) [17] seemed the most plausible explanation; however, experimental observations at Daya Bay [18], RENO [19], and Double Chooz [20] suggest TBM requires corrections to incorporate $\theta_{13} \neq 0$. One such attractive scheme is the trimaximal TM_1 mixing, which is produced by multiplying the TBM mixing matrix by a 23-rotation matrix while keeping intact the first column of the TBM mixing matrix [21–23]. The relationships between the observable in this scheme are as follows

[24],

$$\sin^2\theta_{12} = \frac{1-3\sin^2\theta_{13}}{3\cos^2\theta_{13}}, \tag{2.1}$$

$$\cos\ \delta_{CP} = \frac{(1-5\sin^2\theta_{13})(2\sin^2\theta_{23}-1)}{4\sin\theta_{13}\sin\theta_{23}\sqrt{2(1-3\sin^2\theta_{13})(1-\sin^2\theta_{23})}}. \tag{2.2}$$

TM_1 mixing has proved to be compatible with the global data on neutrino oscillations, in a sense that it includes non-zero θ_{13} and agrees very well with the experiments with its predictions on the mixing angles θ_{13}, θ_{23} and the Dirac CP phase, δ_{CP}.

Over the years, many discrete, symmetry-based studies have been done, which gives rise to TM_1 mixing [24–30]. In the work presented in this chapter, we propose a model constructed using S_4 discrete symmetry within the framework of the minimal seesaw model. The resulting mass matrix leads to TM_1 mixing, and we study its possibility to explain BAU via resonant leptogenesis simultaneously. The choice of right-handed neutrino Majorana mass matrix, M_R, is such that the right-handed neutrinos have degenerate mass at dimension five-level, and successful resonant leptogenesis is achieved by introducing the higher-order term. In other words, our work is based on the extension of the model presented in [31], such that it makes it suitable to study resonant leptogenesis within the minimal seesaw scenario, and the orthogonality condition [23, 25] allows us to realize TM_1 mixing in the leptonic sector.

A study of resonant leptogenesis within the minimal seesaw model based on S_4 symmetry has been carried out in [32]. Unlike the present work, the successful realization of resonant leptogenesis is made possible by radiatively generating the mass splitting among the heavy RHN and the non-zero off-diagonal terms in the Dirac Yukawa-coupling matrix for the models presented in [32]. In their analyses low energy CP violation in neutrino oscillations is absent as a result of the exact TBM structure of the mixing matrix hence, the only source of CP violation comes from the Majorana phases. With the discovery of non-zero θ_{13} [18–20, 33] taken into consideration, we revisit the study of resonant leptogenesis in a minimal seesaw model based on S_4 discrete symmetry that leads to TM_1 mixing. As mentioned earlier, in our work the mass splitting required to achieve successful resonant leptogenesis comes from the symmetry-based breaking term.

The work presented in this chapter is structured as follows. In Section 2.2, we have presented the S_4 flavour symmetric minimal seesaw model followed by a brief description of the features of the S_4 flavour group relevant to the construction of the model. Using the 3σ range of neutrino oscillation data as constraints, we define the allowed region for the model parameters in Section 2.3. In Section 2.4, the framework for resonant leptogenesis is described and the Boltzmann equations, which govern the evolution of the lepton number density and baryon asymmetry parameter, are numerically solved. It also includes the numerical results on neutrinoless double beta decay within the model and we finally conclude our work in Section 2.5.

2.2 Model Framework

The S_4 flavour symmetry has been widely used to explain the observed flavour mixing of neutrinos [21, 29, 31, 34–40]. S_4 group is a non-Abelian discrete group of permutations of four objects. It has 24 elements and 5 irreducible representations 1_1, 1_2, 2, 3_1, and 3_2. The product rules and Clebsch–Gordan coefficients are presented in Appendix A. In this work, we have considered the extension of the standard model (SM) gauge group with a discrete non-abelian group S_4. Additional $Z_3 \times Z_2$ group is introduced to avoid specific unwanted couplings and achieve desired structures for the mass matrices. The two right-handed neutrinos N_1 and N_2, in addition to the SM fermions, are part of the fermion sector. Flavons φ_l, ϕ_l, φ_ν, ϕ_ν, χ, ψ, β, and ρ forms the extension in the scalar sector. The charges carried by the various fields under different symmetry groups are presented in Table 2.1. Following the representations of the fields given in Table 2.1, we can write the invariant Yukawa Lagrangian

Field	$\bar{L}$	e_R	(μ_R, τ_R)	N_1	N_2	H	φ_l	ϕ_l	φ_ν	ϕ_ν	ψ	ξ	ζ
S$_4$	3_1	1_1	2	1_1	1_2	1_1	3_1	3_2	3_1	3_2	3_2	1_1	1_2
Z$_3$	1	ω^2	ω^2	1	1	1	ω	ω	1	1	1	1	1
Z$_2$	1	1	1	-1	1	1	1	1	-1	1	1	1	-1

Table 2.1: Field content and their representations under $S_4\times Z_3\times Z_2$.

$$\begin{aligned}-\mathcal{L} \supset\ & \frac{y_{l_1}}{\Lambda}\bar{L}H\varphi_l e_R + \frac{y_{l_2}}{\Lambda}\bar{L}H\varphi_l(\mu_R,\tau_R) + \frac{y_{l_3}}{\Lambda}\bar{L}H\phi_l(\mu_R,\tau_R)\\ & + \frac{y_{\nu_1}}{\Lambda}\bar{L}\tilde{H}\varphi_\nu N_1 + \frac{y_{\nu_2}}{\Lambda}\bar{L}\tilde{H}\phi_\nu N_2 + \frac{y_{\nu_3}}{\Lambda}\bar{L}\tilde{H}\psi N_2\\ & + y_{N_1}\bar{N}_1^c N_1\beta + y_{N_2}\bar{N}_2^c N_2\beta + y_{N_3}\bar{N}_1^c N_2\rho\frac{\beta\beta}{\Lambda^2} + h.c.,\end{aligned} \tag{2.3}$$

where H is SM Higgs doublet and $\tilde{H} = i\sigma_2 H^*$, σ_2 being the 2$^{\text{nd}}$ Pauli matrices. The vacuum expectation values (vev) of the scalar fields are of the form [31]

$$\langle\varphi_l\rangle = (v_{\varphi_l},0,0),\ \langle\phi_l\rangle = (v_{\phi_l},0,0), \tag{2.4}$$

$$\langle\varphi_\nu\rangle = (0,-v_{\varphi_\nu},v_{\varphi_\nu}),\ \langle\phi_\nu\rangle = (v_{\phi_\nu},v_{\phi_\nu},v_{\phi_\nu}),\ \langle\beta\rangle = v_\beta,\ \langle\rho\rangle = v_\rho. \tag{2.5}$$

As for the vev of ψ we choose $\langle\psi\rangle = (0,-v_\psi,v_\psi)$ following the orthogonality conditions $\langle\psi\rangle\cdot\langle\phi_l\rangle$ and $\langle\psi\rangle\cdot\langle\phi_\nu\rangle$. After electroweak and flavour symmetry breaking, we obtain the following structure for the charged lepton mass matrix

$$m_l = \frac{v_H}{\Lambda}\begin{pmatrix} y_{l_1}v_{\varphi_l} & 0 & 0\\ 0 & y_{l_2}v_{\varphi_l}+y_{l_3}v_{\phi_l} & \\ 0 & 0 & y_{l_2}v_{\varphi_l}-y_{l_3}v_{\phi_l}\end{pmatrix}. \tag{2.6}$$

The charged lepton sector of the model is similar to that of [31] and we similarly assume that the Froggatt-Nielsen mechanism explains the observed mass hierarchy of the charged leptons. Using the vev presented in equation (2.5) for the neutrino sector, we obtain the Dirac and Majorana mass matrix

$$m_D = \begin{pmatrix} 0 & b\\ a & b+c\\ -a & b-c\end{pmatrix} \tag{2.7}$$

and,

$$m_R = \begin{pmatrix} M & 0 \\ 0 & M \end{pmatrix}, \tag{2.8}$$

where $a = y_{\nu_1}\frac{v_H v_{\varphi\nu}}{\Lambda}$, $b = y_{\nu_2}\frac{v_H v_{\phi\nu}}{\Lambda}$, $c = y_{\nu_3}\frac{v_H v_{\psi}}{\Lambda}$ with v_H being the *vev* of the SM Higgs. Taking $y_{N_1} \simeq y_{N_2} = y_N$ we have degenerate masses for the right-handed neutrinos, $M = y_N v_\xi$[1].

In the seesaw framework, the resultant light neutrino mass matrix is given by the well-known formula

$$m_\nu = -m_D m_R^{-1} m_D^T \tag{2.9}$$

and we obtain

$$m_\nu = \frac{1}{M}\begin{pmatrix} b^2 & b(b+c) & b(b-c) \\ b(b+c) & a^2+(b+c)^2 & -(a^2-b^2+c^2) \\ b(b-c) & -(a^2-b^2+c^2) & a^2+(b-c)^2 \end{pmatrix} \tag{2.10}$$

In terms of the re-scaled parameters the light neutrino mass matrix can be written as

$$m_\nu = \begin{pmatrix} b'^2 & b'(b'+c') & b'(b'-c') \\ b'(b'+c') & a'^2+(b'+c')^2 & -(a'^2-b'^2+c'^2) \\ b'(b'-c') & -(a'^2-b'^2+c'^2) & a'^2+(b'-c')^2 \end{pmatrix}, \tag{2.11}$$

with $a' = \frac{a}{\sqrt{M}}$, $b' = \frac{b}{\sqrt{M}}$ and $c' = \frac{c}{\sqrt{M}}$. In charged-lepton diagonal basis, the neutrino mixing matrix, U_ν, is the unitary matrix that diagonalizes the mass matrix in equation (2.11). The resulting U_ν matrix, which is determined entirely from the neutrino sector is

$$U_\nu = U_{\text{TBM}} U_{23} = U_{\text{TM}_1}, \tag{2.12}$$

where U_{TBM} is the tri-bimaximal mixing (TBM) matrix, U_{23} is a unitary matrix whose (1, 2), (1, 3), (2, 1), (3, 1) entries are vanishing and the resulting matrix, U_{TM_1}, has its first column coinciding with that of TBM matrix.

[1] Here we obtain degenerate masses for the right-handed neutrino considering terms upto dimension-5

The diagonalization equation thus reads

$$U_\nu^T m_\nu U_\nu = \mathrm{diag}(m_1, m_2, m_3). \tag{2.13}$$

The light neutrino masses are given as

$$m_1 = 0, \quad m_2 = \frac{1}{2}|(s - \sqrt{t+s^2})|, \quad m_3 = \frac{1}{2}|(s + \sqrt{t+s^2})|, \tag{2.14}$$

where $s = 2a'^2 + 3b'^2 + 2c'^2$ and $t = -24a'^2 b'^2$. It is evident from equation (2.14) that the model predicts normal hierarchy of light neutrino masses.

In the following sections, we have presented the numerical approaches and discussed baryogenesis via resonant leptogenesis, and neutrinoless double beta decay within the context of our model.

2.3 Numerical Analysis

In the previous section, we have shown how the S_4 model can be implemented in the minimal seesaw scenario, producing matrices that lead to TM_1 mixing and normal hierarchy (NH) of masses for the neutrinos. In this section, we perform a numerical analysis to see the model's implication on leptogenesis and other phenomenological predictions. The mass matrix in equation (2.11) gives the effective neutrino mass matrix in terms of the complex model parameters a', b', and c'. We find the allowed region for the model parameters by fitting the model to the current neutrino oscillation data. To do so, we use the 3σ interval [41] for the neutrino oscillation parameters (θ_{12}, θ_{23}, θ_{13}, Δm^2_{21}, Δm^2_{31}) as presented in Table 2.2. A further constraint on the model parameters was applied on the sum of absolute neutrino masses $\sum_i m_i < 0.12$ eV from the cosmological bound [42]. In our analysis, the three complex parameters of the model are treated as free parameters and are allowed to run over the following ranges:

$$|a'| \in [0.1, 0.2]\ \mathrm{eV}^{1/2}, \quad |b'| \in [0.03, 0.06]\ \mathrm{eV}^{1/2}, \quad |c'| \in [10^{-4}, 0.1]\ \mathrm{eV}^{1/2},$$
$$\phi_a \in [-\pi, \pi], \quad \phi_b \in [-\pi, \pi], \quad \phi_c \in [-\pi, \pi],$$

Parameters	Best-fit $\pm 1\sigma$	3σ range
$\Delta m^2_{21}[10^{-5}\text{eV}^2]$	$7.42^{+0.21}_{-0.20}$	$6.82 - 8.04$
$\Delta m^2_{31}[10^{-3}\text{eV}^2]$ (NH)	$2.517^{+0.026}_{-0.028}$	$2.435 - 2.598$
$\sin^2\theta_{12}$	$0.304^{+0.012}_{-0.012}$	$0.269 - 0.343$
$\sin^2\theta_{23}$	$0.573^{+0.016}_{-0.020}$	$0.415 - 0.616$
$\sin^2\theta_{13}$	$0.02219^{+0.00062}_{-0.00063}$	$0.02032 - 0.02410$
δ_{CP}/π (NH)	$1.09^{+0.15}_{-0.13}$	$0.667 - 2.05$

Table 2.2: Neutrino oscillation parameters used to fit the model parameters.

where ϕ_a, ϕ_b, ϕ_c are the phases given by $arg(a')$, $arg(b')$, $arg(c')$, respectively. Using relation $U^\dagger \mathcal{M} U = \text{diag}(m_1^2, m_2^2, m_3^2)$, with $\mathcal{M} = m_\nu m_\nu^\dagger$ and U is a unitary matrix, we numerically diagonalize the effective neutrino mass matrix m_ν. The mixing angles, θ_{23}, θ_{13} are obtained using the relation

$$\sin^2\theta_{23} = \frac{|U_{23}|^2}{1-|U_{13}|^2} \text{ and } \sin^2\theta_{13} = |U_{13}|^2. \tag{2.15}$$

As seen from equations (2.1) and (2.2), TM_1 mixing gives correlations among the mixing angles and CP phases. We have used these relations to calculate the observables θ_{12} and δ_{CP}. The allowed region in the 6-dimensional parameter space corresponds to the observables that satisfy the 3σ bound of the neutrino oscillations experimental data. The minimum of the χ^2-function gives the best-fit values for the model parameters ($|a'|$, $|b'|$, $|c'|$, ϕ_a, ϕ_b, ϕ_c). The χ^2-function is defined as

$$\chi^2 = \sum_i \left(\frac{\lambda_i^{model} - \lambda_i^{expt}}{\Delta\lambda_i} \right)^2, \tag{2.16}$$

where λ_i^{model} is the i^{th} observable predicted by the model, λ_i^{expt} stands for the i^{th} experimental best-fit value (Table 2.2) and $\Delta\lambda_i$ is the 1σ range of the global fit of experimental data for the i^{th} observable. Figures 2.1 and 2.2 show the allowed regions for the different model parameters. Using the function defined in equation (2.16), we have obtained the best-fit values for the parameters $|a'|$, $|b'|$, $|c'|$, ϕ_a,

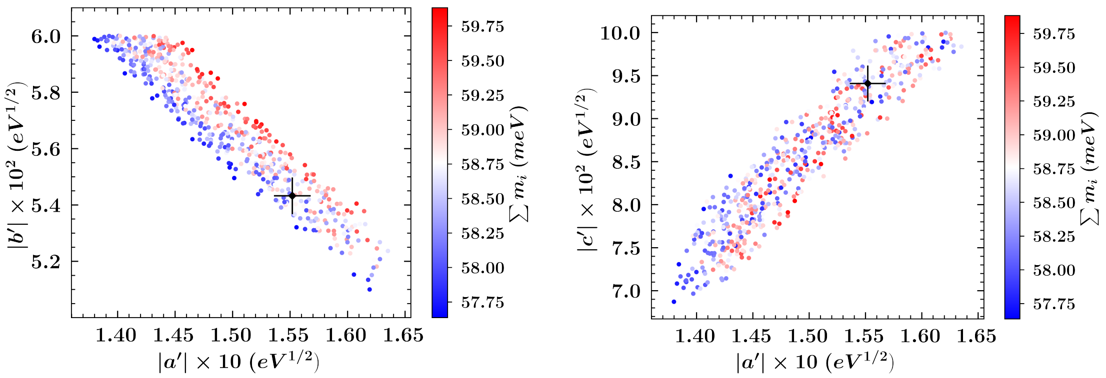

Figure 2.1: Left and right panel shows the correlation of $|a'|$ with $|b'|$ and $|c'|$ respectively along with the variation of $\sum m_i$. The cross mark indicate the best-fit values with $\chi^2 = \chi^2_{min}$, which corresponds to $\sum m_i = 0.0586$ eV.

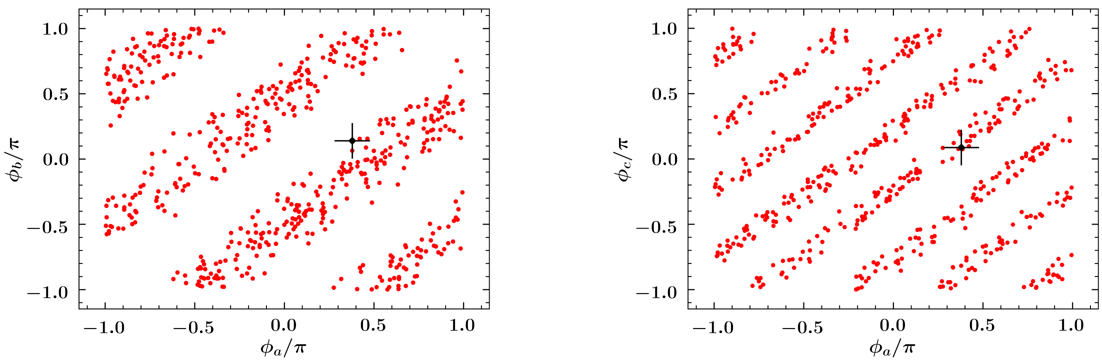

Figure 2.2: Correlation between the phases ϕ_a, ϕ_b and ϕ_c. The cross mark indicates the best-fit values corresponding to χ^2_{min}.

ϕ_b and ϕ_c, which are (0.155, 0.054, 0.09, 0.379π, 0.139π, 0.087π), respectively. A cross mark marks these values in the figure. Additionally, the best-fit values for the neutrino oscillation parameters are $\sin^2\theta_{12} = 0.318$, $\sin^2\theta_{23} = 0.592$, $\sin^2\theta_{13} = 0.02225$, $\sin\delta_{CP} = -0.454$, $\Delta m^2_{21} = 7.25 \times 10^{-5}$ eV^2 and $\Delta m^2_{31} = 2.51 \times 10^{-3}$ eV^2.

2.4 Resonant Leptogenesis

The mechanism of leptogenesis was first proposed by Fukugita and Yanagida to explain the observed baryon asymmetry of the universe (BAU) [13]. In the scenario of thermal leptogenesis with a hierarchical mass spectrum of right-handed neutrinos, the lightest right-handed neutrino must have a mass of at least 10^9 GeV [15]. Although one can lower this limit if their masses are nearly degenerate, the scenario is popularly known as resonant leptogenesis [16, 43]. In this scenario, the one-loop self-energy contribution is resonantly enhanced, resulting in a flavour-dependent asymmetry created by the decay of the right-handed neutrino into a lepton and Higgs is given by [44–48]:

$$\varepsilon_{i\alpha} = \frac{\Gamma\left(N_i \to l_\alpha + H\right) \; - \; \Gamma\left(N_i \to \bar{l}_\alpha + \bar{H}\right)}{\sum_\alpha \Gamma\left(N_i \to l_\alpha + H\right) \; + \; \Gamma\left(N_i \to \bar{l}_\alpha + \bar{H}\right)} \tag{2.17}$$

$$= \sum_{i\neq j} \frac{\mathrm{Im}\left[(Y_\nu^*)_{\alpha i}\,(Y_\nu^*)_{\alpha j}\left(Y_\nu^\dagger Y_\nu\right)_{ij} + \xi_{ij}\,(Y_\nu^*)_{\alpha i}\,(Y_\nu^*)_{\alpha j}\left(Y_\nu^\dagger Y_\nu\right)_{ji}\right]}{\left(Y_\nu^\dagger Y_\nu\right)_{ii}\left(Y_\nu^\dagger Y_\nu\right)_{jj}} \cdot \frac{\xi_{ij}\zeta_j\left(\xi_{ij}^2 - 1\right)}{\left(\xi_{ij}\zeta_j\right)^2 + \left(\xi_{ij}^2 - 1\right)^2}, \tag{2.18}$$

where $\xi_{ij} = M_i/M_j$ and $\zeta_j = \left(Y_\nu^\dagger Y_\nu\right)_{jj}/(8\pi)$ with $Y_\nu = m_D/v$.

In our model, we have two right-handed neutrinos with exactly degenerate masses, $\mathrm{M}_1 = \mathrm{M}_2 = \mathrm{M}$. However, successful resonant leptogenesis requires a tiny mass splitting between the two right-handed neutrinos, which is introduced by adding a higher dimension term in the model (equation (2.3)). Such a term leads to a minor correction in the Majorana mass matrix of equation (2.8), and the resultant structure of the mass matrix may be written as

$$m_R = \begin{pmatrix} M & \epsilon \\ \epsilon & M \end{pmatrix}, \tag{2.19}$$

where $\epsilon = y_{N_3} v_\rho \frac{v_\beta^2}{\Lambda^2}$ is a parameter that quantifies the tiny difference between masses required for leptogenesis [2]. The mass matrix in equation (2.19) is diagonalized using a (2×2) matrix of the form

$$U_R = \frac{1}{\sqrt{2}} \begin{pmatrix} 1 & 1 \\ -1 & 1 \end{pmatrix}, \tag{2.20}$$

[2] ϵ is assumed to be real.

with real eigenvalues $\mathrm{M}_1 = \mathrm{M} - \epsilon$ and $\mathrm{M}_2 = \mathrm{M} + \epsilon$. In the basis where the charged-lepton and Majorana mass matrix are diagonal, the Dirac mass matrix (equation (2.7)) takes the form

$$m'_D = \frac{1}{\sqrt{2}} \begin{pmatrix} -b & b \\ a-(b+c) & a+(b+c) \\ -a-(b-c) & -a+(b-c) \end{pmatrix}. \tag{2.21}$$

From this point onward, we will take $Y_\nu = m'_D/v$, which is relevant for calculating CP asymmetry that arises during the decay of right-handed neutrinos in an out-of-equilibrium way. Taking the best-fit values of the model parameters obtained in the previous section, we solve the following coupled Boltzmann equations describing the evolution, with respect to $z = \mathrm{M}_1/T$, of RH neutrino density, N_{N_i} and lepton number density for three flavours, $N_{\alpha\alpha}$ corresponding to $\alpha = e,\ \mu,\ \tau$ [16, 47].

$$\frac{dN_{N_i}}{dz} = -D_i \left(N_{N_i} - N_{N_i}^{\mathrm{eq}}\right) \tag{2.22}$$

$$\begin{aligned} \frac{dN_{\alpha\alpha}}{dz} &= -\sum_{i=1}^{2} \varepsilon_{i\alpha} D_i \left(N_{N_i} - N_{N_i}^{\mathrm{eq}}\right) \\ &\quad - \frac{1}{4}\left\{\sum_{i=1}^{2} (rz)^2 D_i \mathcal{K}_2(rz) + W_{\Delta L=2}\right\} N_{\alpha\alpha}. \end{aligned} \tag{2.23}$$

The following equation gives the equilibrium number density of N_i,

$$N_{N_i}^{\mathrm{eq}} = \frac{45 g_N}{4\pi^4 g_*} z^2 \mathcal{K}_2(z), \tag{2.24}$$

with $\mathcal{K}_{1,2}(z)$ being the modified Bessel function. The parameter, D_i, sometimes called the decay parameter is defined as

$$D_i = \frac{z}{H(z=1)} \frac{\Gamma_{N_i}}{N_{N_i}^{\mathrm{eq}}}, \tag{2.25}$$

which gives the total decay rate with respect to Hubble rate and $W_{\Delta L=2}$ denotes the washout coming from $\Delta L = 2$ scattering process[3].

[3]Such processes are explained in [16]

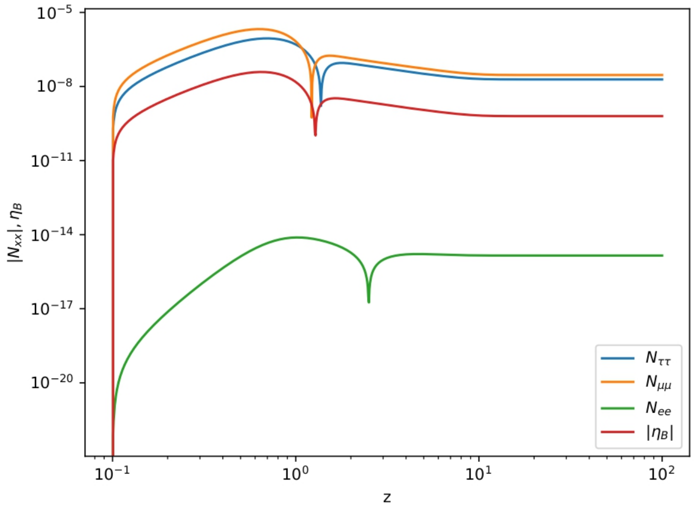

Figure 2.3: Variation of lepton number density for three flavours and baryon asymmetry parameter, η_B as a function of z.

We take $M_1 = 10$ TeV and $d = (M_2 - M_1)/M_1 \simeq 10^{-8}$ in order to estimate the value of BAU. We made the calculations related to baryon asymmetry using the ULYSSES package [49]. Figure 2.3 shows the evolution of three flavoured lepton number density, $N_{\alpha\alpha}$ and baryon asymmetry, η_B as a function of $z = \mathrm{M}_{N_1}/T$. The asymptotic value suggests that the obtained value of baryon asymmetry is $|\eta_B| \approx 6.3 \times 10^{-10}$.

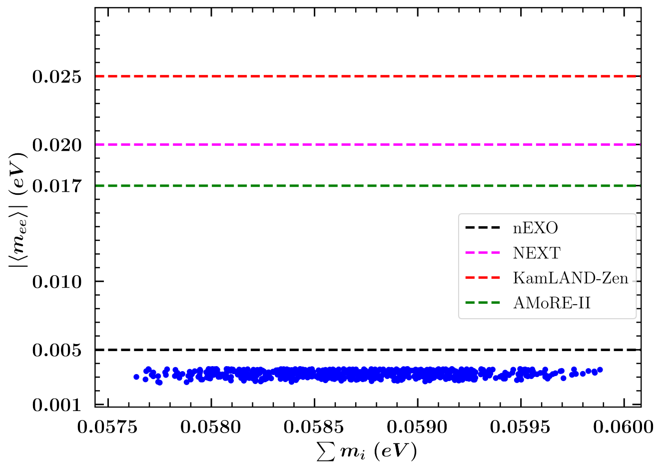

Figure 2.4: The predicted values of $|\langle m_{ee}\rangle|$ with respect to $\sum m_i$.

The effective Majorana mass relevant for the neutrinoless double beta decay ($0\nu\beta\beta$) is the (1, 1) element of the effective neutrino mass matrix (equation 8), $|\langle m_{ee}\rangle| = |(m_\nu)_{11}|$. Figure 2.4 shows the predicted values of $|\langle m_{ee}\rangle|$ with respect to $\sum m_i$ for the allowed region of parameter space. We have also shown the sensitivity reach of some experiments such as nEXO [50], KamLAND-Zen [51], NEXT [52], AMoRE-II [53]. It shows that $|\langle m_{ee}\rangle|$ ranges from 2.6 meV to 3.6 meV and probing such small parameters by ($0\nu\beta\beta$) experiments would be quite difficult.

2.5 Conclusion

We have explored the S_4 symmetric flavour model in the context of a minimal Type-I seesaw mechanism leading to TM_1 mixing pattern in the leptonic sector. To achieve TM_1 mixing, we extended the scalar sector further by adding a flavon ψ and its *vev* is chosen such that it follows the orthogonality conditions (i.e., $\langle\psi\rangle\cdot\langle\phi_l\rangle$ and $\langle\psi\rangle\cdot\langle\phi_\nu\rangle$). The resulting effective neutrino mass matrix predicts NH for masses of the neutrinos and 0.0576 eV $< \sum m_i <$ 0.0599 eV. An allowed region for the model parameters is calculated numerically to ensure that the predicted mixing angles, CP phase, and mass squared differences fall within the 3σ bounds of current oscillation data. Among various points within the 6-dimensional parameter space, the best-fit value is obtained through chi-squared analysis. After analyzing the obtained parameter space, we determined that the effective Majorana neutrino mass, $|\langle m_{ee}\rangle|$, is relatively small and difficult to detect in $0\nu\beta\beta$ experiments.

Furthermore, we investigated baryogenesis via flavoured resonant leptogenesis. The right-handed neutrinos are degenerate at the dimension 5 level, and hence a tiny splitting was generated by including a higher dimension term. We have taken the splitting parameter, $d \simeq 10^{-8}$, and thus, obtained a non-zero, resonantly enhanced CP asymmetry from the out-of-equilibrium decay of right-handed Majorana neutrinos. The analysis of the evolution of particles and asymmetry is done by solving the Boltzmann equations. Here, the best-fit values for the model parameters is considered as inputs, and the Boltzmann equations are solved numerically to estimate baryon asymmetry. It was found that the predicted baryon asymmetry comes out to be $|\eta_B| \approx 6.3 \times 10^{-10}$.

Bibliography

[1] Group, P. D. *et al.* Review of particle physics. *Progress of Theoretical and Experimental Physics* **2020** (8), 083C01, 2020.

[2] Aker, M. *et al.* Improved upper limit on the neutrino mass from a direct kinematic method by KATRIN. *Physical review letters* **123** (22), 221802, 2019.

[3] Faessler, A. Status of the determination of the electron-neutrino mass. *Progress in Particle and Nuclear Physics* 103789, 2020.

[4] Araki, T. *et al.* Measurement of neutrino oscillation with KamLAND: Evidence of spectral distortion. *Physical Review Letters* **94** (8), 081801, 2005.

[5] Cao, S. *et al.* Physics potential of the combined sensitivity of T2K-II, NOνA extension, and JUNO. *Physical Review D* **103**, 112010, 2021.

[6] Nath, A. & Francis, N. K. Detection techniques and investigation of different neutrino experiments. *International Journal of Modern Physics A* **36** (13), 2130008, 2021.

[7] Minkowski, P. $\mu \rightarrow$ eγ at a rate of one out of 109 muon decays? *Physics Letters B* **67** (4), 421–428, 1977.

[8] Yanagida, T. Horizontal symmetry and masses of neutrinos. *Progress of Theoretical Physics* **64** (3), 1103–1105, 1980.

[9] Mohapatra, R. N. Mechanism for understanding small neutrino mass in superstring theories. *Physical Review Letters* **56** (6), 561, 1986.

[10] Ma, E. Verifiable radiative seesaw mechanism of neutrino mass and dark matter. *Physical Review D* **73** (7), 077301, 2006.

[11] Mohapatra, R. N. *et al.* Neutrino masses and oscillations in models with large extra dimensions. *Physics Letters B* **466** (2-4), 115–121, 1999.

[12] Arkani-Hamed, N. *et al.* Neutrino masses from large extra dimensions. *Physical Review D* **65** (2), 024032, 2001.

[13] Fukugita, M. & Yanagida, T. Barygenesis without grand unification. *Physics Letters B* **174** (1), 45–47, 1986.

[14] Kuzmin, V. A. *et al.* On anomalous electroweak baryon-number non-conservation in the early universe. *Physics Letters B* **155** (1-2), 36–42, 1985.

[15] Davidson, S. & Ibarra, A. A lower bound on the right-handed neutrino mass from leptogenesis. *Physics Letters B* **535** (1-4), 25–32, 2002.

[16] Pilaftsis, A. & Underwood, T. E. Resonant leptogenesis. *Nuclear Physics B* **692** (3), 303–345, 2004.

[17] Harrison, P. F. *et al.* Tri-bimaximal mixing and the neutrino oscillation data. *Physics Letters B* **530** (1-4), 167–173, 2002.

[18] An, F. *et al.* Observation of electron-antineutrino disappearance at Daya Bay. *Physical Review Letters* **108** (17), 171803, 2012.

[19] Ahn, J. K. *et al.* Observation of reactor electron antineutrinos disappearance in the RENO experiment. *Physical Review Letters* **108** (19), 191802, 2012.

[20] Abe, Y. *et al.* Indication of reactor electron antineutrinos disappearance in the Double Chooz experiment. *Physical Review Letters* **108** (13), 131801, 2012.

[21] Luhn, C. Trimaximal TM_1 neutrino mixing in S_4 with spontaneous CP violation. *Nuclear Physics B* **875** (1), 80–100, 2013.

[22] Grimus, W. Discrete symmetries, roots of unity, and lepton mixing. *Journal of Physics G: Nuclear and Particle Physics* **40** (7), 075008, 2013.

[23] Rodejohann, W. & Zhang, H. Simple two parameter description of lepton mixing. *Physical Review D* **86** (9), 093008, 2012.

[24] de Medeiros Varzielas, I. & Lavoura, L. Flavour models for TM_1 lepton mixing. *Journal of Physics G: Nuclear and Particle Physics* **40** (8), 085002, 2013.

[25] Antusch, S. *et al.* Trimaximal mixing with predicted θ_{13} from a new type of constrained sequential dominance. *Nuclear Physics B* **856** (2), 328–341, 2012.

[26] King, S. F. Minimal see-saw model predicting best-fit lepton mixing angles. *Physics Letters B* **724** (1-3), 92–98, 2013.

[27] Chakraborty, M. *et al.* Predictive S_4 flavon model with TM_1 mixing and baryogenesis through leptogenesis. *Journal of High Energy Physics* **2020** (9), 1–48, 2020.

[28] King, S. F. *et al.* Lepton mixing predictions from Δ $(6n^2)$ family symmetry. *Physics Letters B* **726** (1-3), 312–315, 2013.

[29] King, S. F. Littlest seesaw. *Journal of High Energy Physics* **2016** (2), 85, 2016.

[30] Xing, Z.-z. & Zhou, S. Tri-bimaximal neutrino mixing and flavor-dependent resonant leptogenesis. *Physics Letters B* **653** (2-4), 278–287, 2007.

[31] Zhao, Z.-h. Realizing tri-bimaximal mixing in minimal seesaw model with S_4 family symmetry. *Physics Letters B* **701** (5), 609–613, 2011.

[32] Nguyen, T. P. *et al.* Radiatively generated leptogenesis in flavor symmetry models. *Advances in High Energy Physics* **2012**, 2012.

[33] Adamson, P. *et al.* Improved search for muon-neutrino to electron-neutrino oscillations in MINOS. *Physical Review Letters* **107** (18), 181802, 2011.

[34] Koide, Y. S_4 flavor symmetry embedded into SU(3) and lepton masses and mixing. *Journal of High Energy Physics* **2007** (08), 086, 2007.

[35] Krishnan, R. *et al.* Simplest neutrino mixing from S_4 symmetry. *Journal of High Energy Physics* **2013** (4), 1–15, 2013.

[36] Brown, T. *et al.* Neutrino masses, mixing, and oscillations in the S_4 model of permutation symmetry. *Physical Review D* **30** (1), 255, 1984.

[37] Bazzocchi, F. *et al.* Fermion masses and mixings in a S_4 based model. *Nuclear Physics* **816**, 204–226, 2009.

[38] Björkeroth, F. *et al.* A natural $S_4 \times SO(10)$ model of flavour. *Journal of High Energy Physics* **2017** (10), 1–28, 2017.

[39] Meloni, D. A see-saw S_4 model for fermion masses and mixings. *Journal of Physics G: Nuclear and Particle Physics* **37** (5), 055201, 2010.

[40] Chen, P.-T. *et al.* A new littlest seesaw model. *Journal of Physics G: Nuclear and Particle Physics* **47** (6), 065001, 2020.

[41] Esteban, I. *et al.* The fate of hints: updated global analysis of three-flavor neutrino oscillations. *Journal of High Energy Physics* **2020** (9), 1–22, 2020.

[42] Aghanim, N. *et al.* Planck 2018 results-VI. cosmological parameters. *Astronomy & Astrophysics* **641**, A6, 2020.

[43] Pilaftsis, A. CP violation and baryogenesis due to heavy majorana neutrinos. *Physical Review D* **56** (9), 5431, 1997.

[44] Xing, Z.-z. & Zhang, D. Bridging resonant leptogenesis and low-energy CP violation with an RGE-modified seesaw relation. *Physics Letters B* **804**, 135397, 2020.

[45] Pilaftsis, A. Resonant CP violation induced by particle mixing in transition amplitudes. *Nuclear Physics B* **504** (1-2), 61–107, 1997.

[46] Anisimov, A. *et al.* The CP-asymmetry in resonant leptogenesis. *Nuclear Physics B* **737** (1-2), 176–189, 2006.

[47] De Simone, A. & Riotto, A. On resonant leptogenesis. *Journal of Cosmology and Astroparticle Physics* **2007** (08), 013, 2007.

[48] Francis, N. K. & Singh, N. N. Validity of quasi-degenerate neutrino mass models and their predictions on baryogenesis. *Nuclear Physics B* **863** (1), 19–32, 2012.

[49] Granelli, A. *et al.* ULYSSES: Universal LeptogeneSIS Equation Solver. *Computer Physics Communications* **262**, 107813, 2021.

[50] Licciardi, C. *et al.* The sensitivity of the nEXO experiment to majorana neutrinos. In *Journal of Physics: Conference Series*, vol. 888. 012237, IOP Publishing, 2017.

[51] Obara, S. *et al.* Status of balloon production for KamLAND-Zen 800 kg phase. *Nuclear Instruments and Methods in Physics Research Section A: Accelerators, Spectrometers, Detectors and Associated Equipment* **845**, 410–413, 2017.

[52] Gómez Cadenas, J. J. *et al.* Present status and future perspectives of the NEXT experiment. *Advances in High Energy Physics* **2014**, 2014.

[53] Bhang, H. *et al.* AMoRE experiment: a search for neutrinoless double beta decay of ^{100}Mo isotope with ^{40}Ca^{100}MoO$_4$ cryogenic scintillation detector. In *Journal of Physics: Conference Series*, vol. 375 issue 4. 042023, IOP Publishing, 2012.